JOURNAL OF MECHANICAL ENGINEERING AND SCIENCES (JMES)
ISSN: 2289-4659 e-ISSN: 2231-8380
VOL. 14, ISSUE 3, 7049 – 7057
DOI: https://doi.org/10.15282/jmes.14.3.2020.07.0552

ORIGINAL ARTICLE

Effect of strain energy on the grain growth behaviour of ultrafine-grained iron-chromium alloy by equal channel angular pressing

M. Rifai[1], H. Miyamoto[2]

[1] Center of Science and Technology for Advanced Material, National Nuclear Energy Agency, Kawasan Puspiptek, Serpong, Tangerang 15314, Indonesia
Phone: +6281331009991
[2] Department of Mechanical Engineering, Doshisha University, 1-3 Tatara Miyakodani, Kyotanabe, Kyoto 610-0394, Japan

ABSTRACT – The grain growth of an ultrafine-grained iron-chromium alloy has been investigated focusing on the early stage of restoration of strain. Ultrafine-grained (UFG) material has been prepared by equal channel angular pressing (ECAP) up to eight passes via route Bc. The post-ECAP annealing process was completed from 473 until 1373 K for one hour. The microstructure and hardness were then analyzed by electron back-scattering diffraction, transmission electron microscope, X-ray diffractometer and microhardness. The hardness after post-ECAP annealing exhibited the typical three-stages softening. Namely, the hardness remained stable after the annealing temperature up to 698 K and then declined significantly until the temperature of 973 K. Finally, hardness remained stable again at a higher temperature. In the second stage, grains grew uniformly, which differ from the typical nucleation-and-growth mode of discontinuous recrystallization. It was found by X-ray line broadening analysis that strain was released in the early stage prior to the significant softening stage. It was suggested that the homogeneous grain growth was led by the uniform grain distribution with a high angle grain boundaries fraction.

ARTICLE HISTORY
Revised: 19th Mar 2020
Accepted: 25th Mar 2020

KEYWORDS
Low carbon steel;
ECAP;
annealing behaviour;
grain growth

INTRODUCTION

Equal channel angular pressing (ECAP) is a severe plastic deformation (SPD) technique, which imposes high plastic strain and leads to a significant grain refinement to sub micrometres and nanometers [1]. Grain refinement by ECAP has more advantages than conventional material processes for strengthening materials in a bulk form for structural applications since it does not require an alloying element and can be applied to essentially all kinds of metals. ECAP can generate ultrafine grain (UFG) structure with a high fraction of high angle grain boundaries [2].

UFG structures have been regarded as partially deformation structure as well as UFG structure. Namely, UFG structures by ECAP are considered to have stored residual dislocations in grain or at grain boundaries. Such grain boundaries with extrinsic grain boundary dislocations are called non-equilibrium grain boundaries, and they are considered to be the origin of unique mechanical, physical and chemical properties [1-3]. This study will contribute to the application at biomedical, automotive purposes.

Thermal stability of UFG materials is an important property along with mechanical properties. The annealing behaviour of the UFG material has been investigated, such as copper [4], aluminium, and its alloy [5], titanium [6], iron [7], and low carbon steel [8, 9]. It was reported that the thermal stability of the microstructure of the ECAP processed face-centred cubic (FCC) metals are low, and in general grains grow apparently by the mode of so-called abnormal grain growth [10, 11], where a small fraction of grains grow preferentially replacing other grains [12]. However, this growth behaviour can be regarded as the so-called discontinuous recrystallization with nucleation and its growth process since ECAP processed UFG structure is partially deformation structure. In other words, growing grains in UFG can be regarded as a nucleus. In this context, it is effective to create the dislocation-free UFG with equilibrium grain boundaries and examine annealing behaviour focusing on the early stage of grain growth in order to clarify the origin of low thermal stability and abnormal grain growth. Such knowledge can contribute to creating the UFG materials with high thermal stability, but there is no publication which explains the body-centred cubic (BCC) metallic materials.

Pure metals of BCC is intrinsically fast to be recovered and may exhibit different annealing behaviour from FCC counterparts [13, 14]. Namely, one can expect to obtain dislocation-free UFG by appropriate annealing, which avoids grain growth [15]. However, annealing behaviour of UFG of pure BCC alloy has not been investigated focusing on the early stage of restoration of strain. The stored dislocation can be analyzed through the transmission electron microscope (TEM) or X-ray line broadening analysis. The X-ray line broadening analysis corresponded to grain refinement and dislocation density [16]. In this study, annealing behaviour on UFG structure of iron-chromium alloy as BCC metallic material has been investigated in order to examine the origin of low thermal stability of UFG ECAP processed materials.

*CORRESPONDING AUTHOR | M. Rifai | ✉ mrifai@batan.go.id

© The Authors 2020. Published by Penerbit UMP. This is an open access article under the CC BY license.

METHODS AND MATERIALS

The present material had a chemical composition of iron-chromium with Cr 20.03; C 0.0004; N 0.0013 and Fe balance (in mass per cent). This alloy was machined with dimensions of 8 mm × 8 mm × 120 mm for ECAP pressing. ECAP procedures were carried out using a split die with two channels intersecting at an inner angle of 90° and an outer angle of 0° at 423 K. Before the ECAP process, the samples were lubricated with a high-temperature fluorine lubricating grease and then pressed for eight passes via routes Bc. An ECAP die set with an internal angle, Φ of 90° and outer angle, Ψ of 0° was assembled. This setting contributed an equivalent strain of 1.15 of each pressing using the following equation [17]:

$$\varepsilon = \frac{1}{\sqrt{3}}\left[2\cot\left(\frac{\Phi}{2}+\frac{\Psi}{2}\right)+\Psi\,\mathrm{cosec}\left(\frac{\Phi}{2}+\frac{\Psi}{2}\right)\right] \quad (1)$$

After ECAP, billets were annealed using infrared furnace (ULVAC MILA5000) from 473 to 1373 K in a vacuum for one hour. Details of the ECAP procedure have been previously published [12]. Mechanical properties were measured by hardness. The microhardness experiments were performed on a Vickers hardness testing machine under a load, for 15 s dwell time for each annealing temperature. Hardness testing was carried out for ten times per each sample. And then, microstructure observation was carried out by a scanning electron microscope of field-emission type (FE-SEM, JSM 7001F), equipped with electron back-scattered diffraction (EBSD, Oxford Instrument Co.) image, and a transmission electron microscope (TEM, JEM 2100F). Therefore, EBSD orientation maps were processed using INCA™ software. TEM sample preparation was needed. Thin foils for TEM were polished using abrasive papers to about 100 μm in thickness and then thinned by a twin-jet polishing Tenupol 5 facility using a solution of 40% acetic acid, 30% phosphoric acid, 20% nitric acid, and 10% distilled water. X-ray diffraction (XRD) on ECAP processed and post-annealing sample was carried out by SmartLab, Rigaku. XRD samples surface was polished by an automatic polisher. The SmartLab X-ray diffractometer used CuKα, 40 kV, 200 mA from 30° until 120° with a continuous scanning type. Full width half maximum (FWHM) and integral breadth were determined after fitting the scattered XRD data. Detail regarding the setup for microstructure observation, XRD, and microhardness testing are available in our previous publication.

RESULTS AND DISCUSSION

In the previous result on the degradation of corrosion resistance in the early stage of annealing is attributed to stability change of by recovering of dislocation structure inside grains and non-equilibrium grain boundaries by ECAP. This corrosion properties study may be related to grain growth behaviour which can be used for explaining the high passivation stability of iron-chromium alloy [12].

The effect of annealing temperature on microhardness has been previously reported. The microhardness results showed three stages of softening with increasing annealing temperature [12, 18]. The hardness was steady up to 698 K and then decreased gradually until 973 K. Finally, hardness became steady again. UFG structure can be seen in the ECAP processed sample, and grain size remained constant until 698 K. It corresponds within the first stage of softening [12]. Appreciable grain growth was observed to occur homogeneously at a temperature higher than 698 K. It corresponded with the second stage of appreciable softening in Figure 1.

Grain boundary misorientation maps on ECAP and after post-ECAP annealing from 473 – 1373 K are represented in Figure 1. High angle grain boundaries (HAGB) fraction on ECAP processed microstructure is predominant with a little fraction of low angle grain boundary (LAGB) [19]. Because of low orientation resolution, boundaries with misorientation smaller than 2° was omitted. Homogeneous microstructure evolution with small equiaxed grains and high HAGB fraction was exhibited on post-ECAP annealing sample until 698 K. However, grain size increased gradually until the annealing temperature of 1373 K, but HAGB fraction almost remained constant.

Distribution of misorientation angle was obtained from EBSD observation after ECAP and post-ECAP annealing, as shown in Figure 2. Result of as-ECAP processed materials shows boundary misorientation with a peak in the range of 2° - 5° with low HAGB misorientation distribution [20]. After 773 K annealed temperature, the difference in misorientation distribution became noticeable. Misorientation distribution of this alloy shows one small peak at low and high angle misorientation.

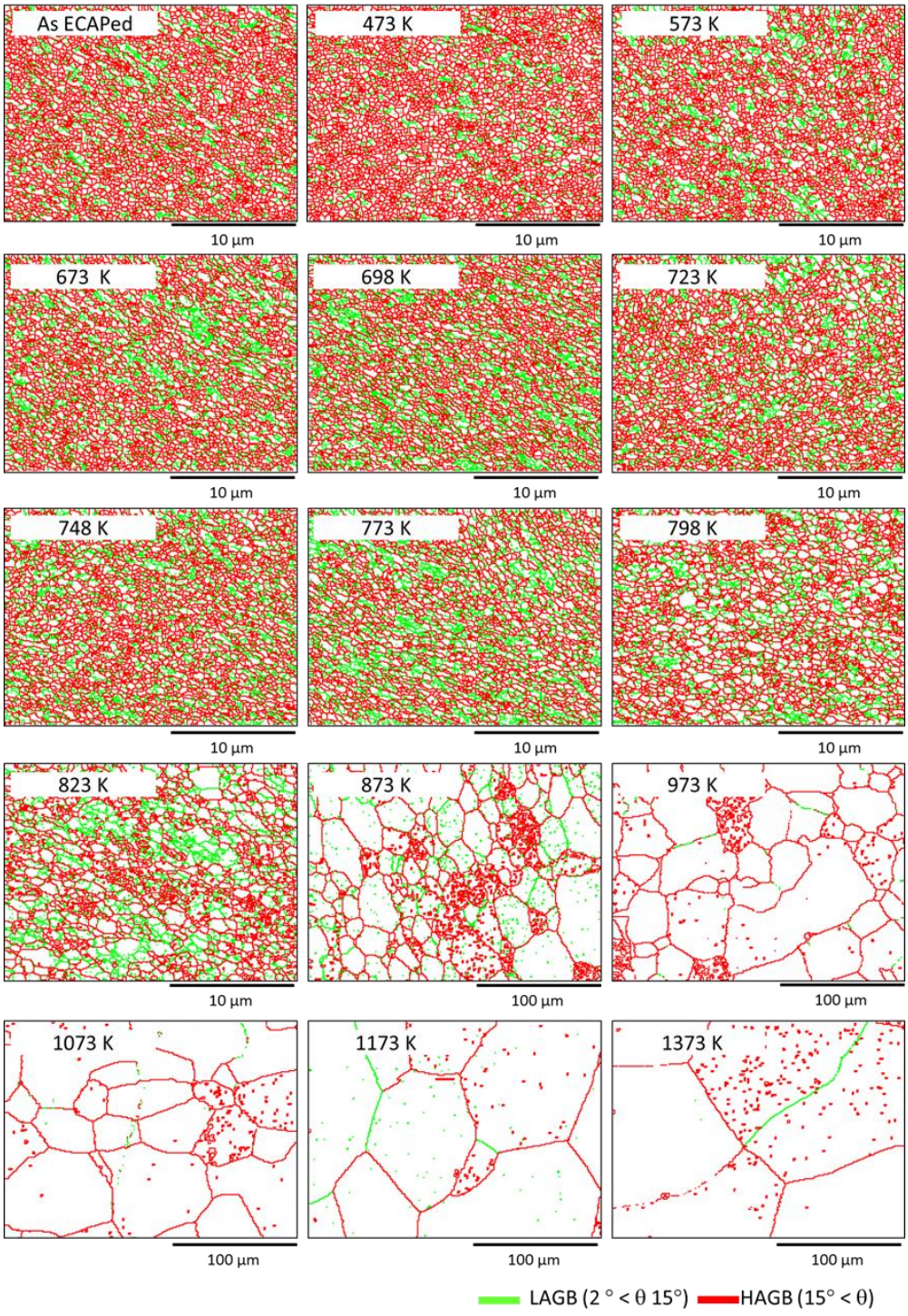

Figure 1. Misorientation image map by EBSD after the post-ECAP annealing

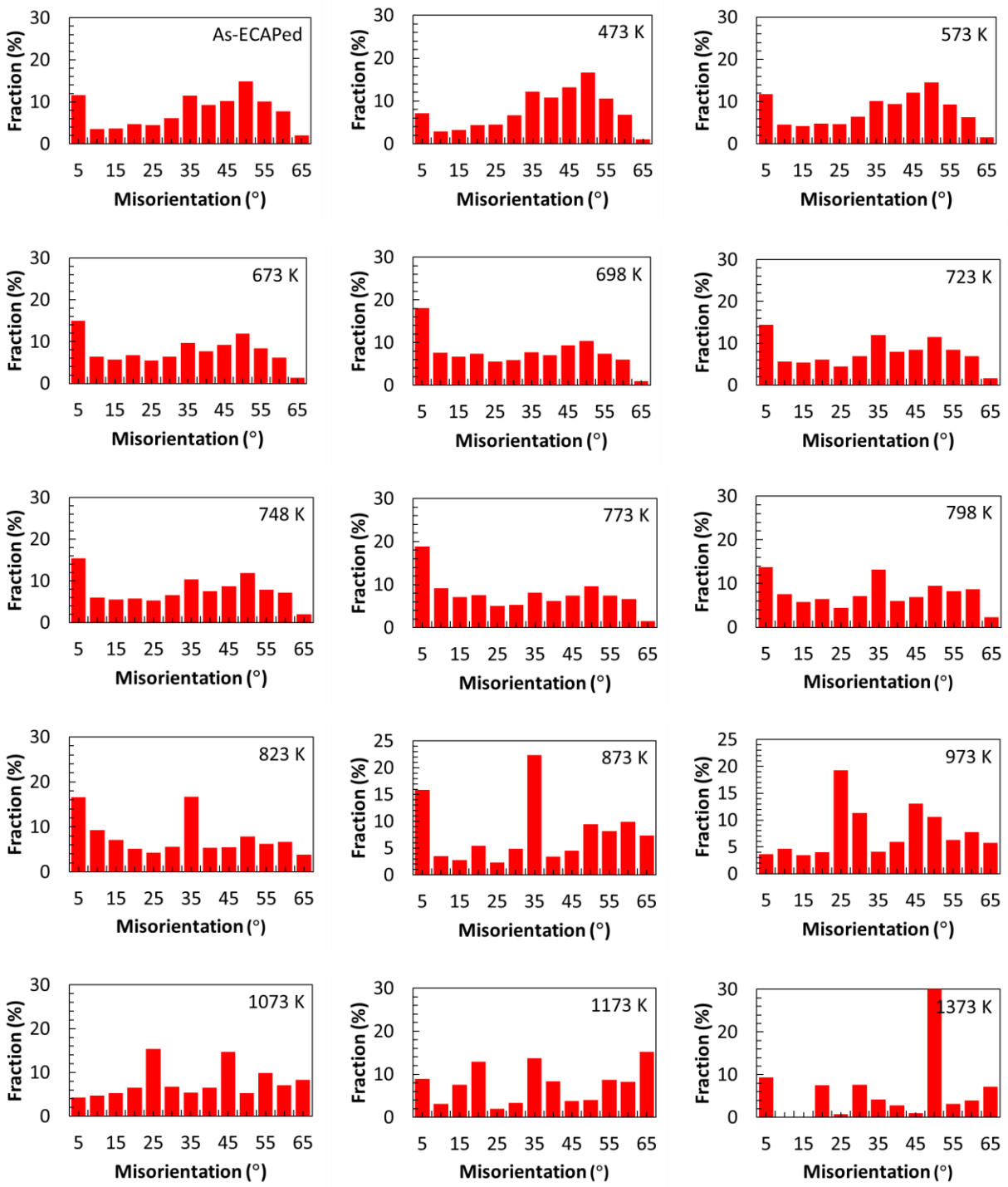

Figure 2. Distribution misorientation by EBSD after the post-ECAP annealing

The microstructure of TEM was also observed on ECAP and after post-ECAP annealing up to 823 K, as shown in Figure 3. Under the annealing temperature of 698 K, due to the recovery stage, there was not much difference in microstructure from the eight passes ECAP. The microstructure of the ECAP processed sample exhibited a dark contrast compared to that of the post-ECAP annealing; it indicates that the dislocation was kept inside the UFG structure. The light contrast appeared at the TEM micrograph of the post-ECAP annealing due to the releasing of dislocation in grains. The boundary spacing remained constant up to the annealing temperature of 698 K, and then gradually increased as the annealing temperature increased, as shown in Figure 4.

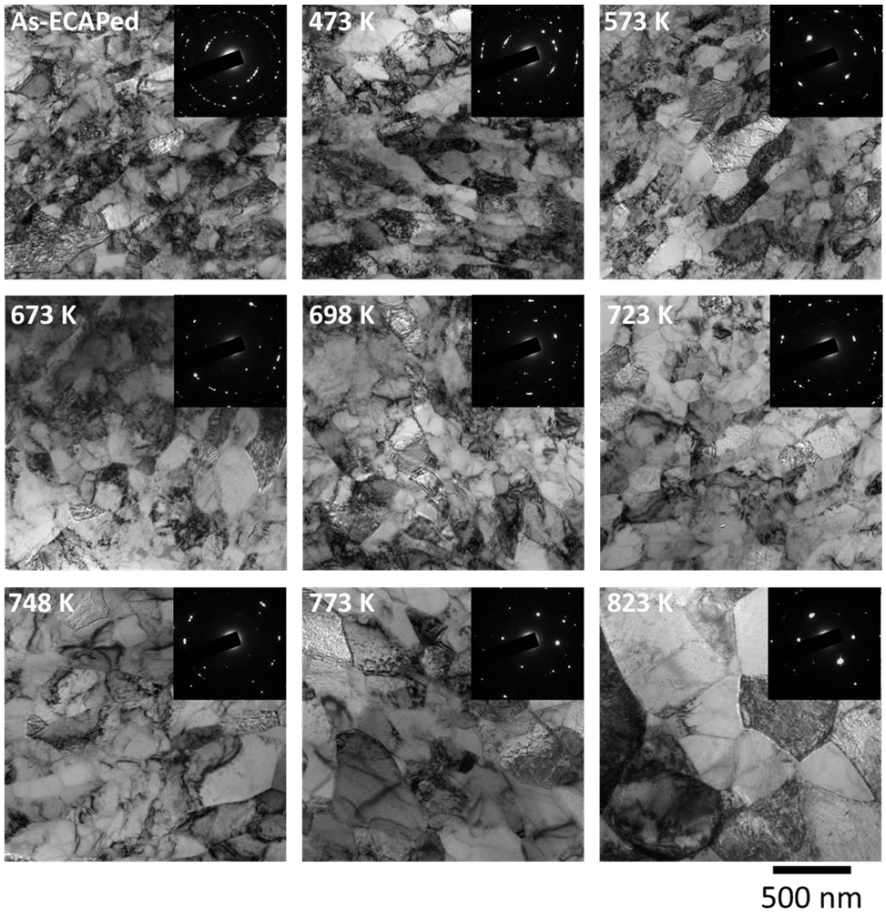

Figure 3. TEM micrograph after the post-ECAP annealing

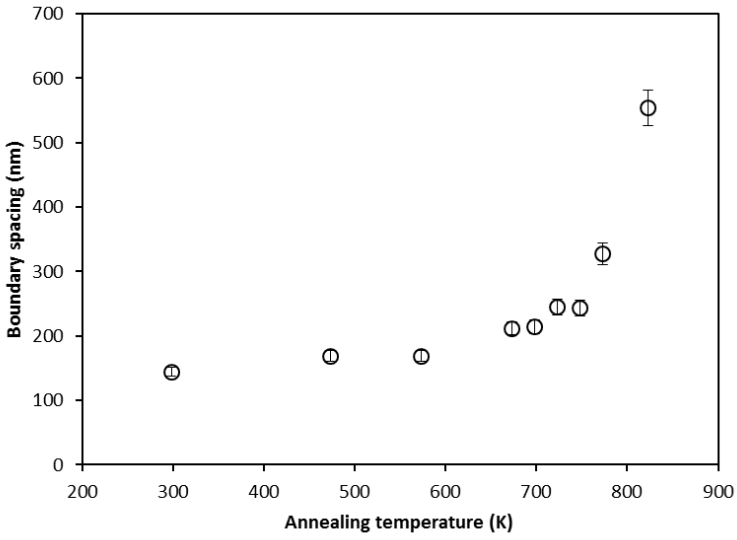

Figure 4. Boundary spacing of the post-ECAP annealing

One of the methods for identifying dislocation density is X-ray line broadening by XRD [12]. X-ray line broadening of the ECAP processed sample can be observed significantly in the previous report [12]. It became smaller with the increasing annealing temperature. This line broadening can be used for measuring coherent domain size, D and microstrain, ε due to the broadening of XRD data line [21]. The calculation of dislocation density, ρ is contributed by the relationship at Eq. 2 [21]:

$$(\beta \cos \theta/\lambda)^2 = (1/D)^2 + (4\varepsilon \sin \theta/\lambda)^2 \quad (2)$$

The D, ε and ρ values of different annealing temperature can be seen in Figure 5.

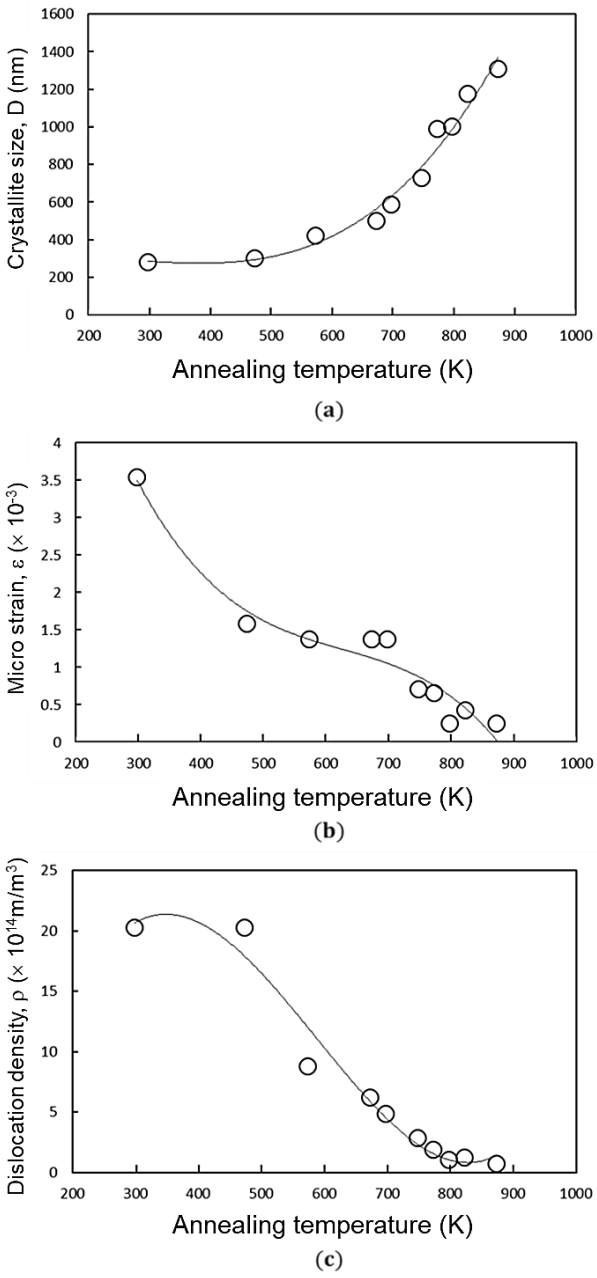

Figure 5. Effect of annealing temperature on (a) crystallite size, (b) microstrain and (c) dislocation density

The line broadening analysis obtained crystallite size, microstrain, and dislocation density in this report, seen in Figure 5. The crystallite size increased with the increasing annealing temperature. On the other hand, microstrain and dislocation density decreased with the increasing annealing temperature [12].

During the annealing temperature, material softening occurred gradually and uniformly in a fixed time. This behaviour was similar to the softening behavior of aluminium alloys which inhibits discontinuous recrystallization by extended recovery stage [22]. Strain energy stored as dislocations can be released in recovery process easily prior to recrystallization [12]. Consequently, strain energy accumulated and stored in UFG structures in the as-ECAP state may be released prior to the next stage, resulting in the formation of UFG structure with less stored strain energy [12]. Homogeneous grain size distribution with a high fraction of HAGB (81%) may lead to homogeneous and normal grain growth whose driving force is solely grain boundary energy [22], rather than recrystallization which requires strain energy as driving force [12].

This grain growth process is different from the common material in the FCC material such as aluminium alloys [5], copper [23], nickel [24] and austenitic stainless steels [25]. The abnormal grain growth in FCC material shows small

fractions of grains growing predominantly, replacing the other smaller, Phenomenologically, this mode of grain growth can be regarded as discontinuous recrystallization [7]. The material processed by ECAP is considered by high internal stresses, which are related to both high dislocation densities and non-equilibrium grain boundaries [1, 26–28]. Microstructure with high HAGB fraction have been recommended as being basically resistant to discontinuous recrystallization regardless of an apparently high stored energy, and only the uniform grain growth tends to operate frequently in such structures [29, 30].

In the pure BCC, the material showed the release strain energy stored as dislocations density in recovery process prior to the recrystallization process [12]. In this regard, the strain energy that was stored in UFG structure was released earlier and this early recovery of strain affected the mode grain growth in annealing. Humphreys et al. [22] explained that annealing phenomena might occur in two ways. The annealing phenomena occur heterogeneously throughout the material and formally described in terms of nucleation and growth stages, and in this case, they are described as discontinuous processes [31]. On the other hand, the annealing phenomena may occur homogeneously and evolve gradually with no identifiable nucleation and growth stages in the microstructure and in this case, they are described as continuous processes. The continuous annealing phenomena include recovery by subgrain growth, continuous recrystallization and normal grain growth and the discontinuous annealing phenomena include discontinuous subgrain growth, primary recrystallization and abnormal grain growth [32, 33].

The homogeneous and normal grain growth behaviour can be expressed by the following in terms of activation energy during the annealing process can be determined using the following equation [32, 33]:

$$d^{1/N} - d_o^{1/N} = K_o t \, exp\left(-\frac{Q}{RT}\right) \tag{3}$$

where d_0 is the initial grain size; d is the grain size after annealing; N is a constant usually taken as unity; K_0 is a temperature-dependent constant; t is the annealing time; Q is the activation energy for grain growth; R is the gas constant, and T is the annealing temperature. The activation energy for grain growth was achieved by constructing a semi-logarithmic plot $\left(d^{1/N} - d_o^{1/N}\right)$ versus, $1/\mathrm{T}$ as shown in Figure 6. The slopes corresponding to activation energies shows two different slopes at the low and high-temperature regime. At low-temperature regime, the low activation of 148 kJ/mol that closes to the activation energy of grain boundary diffusion, may correspond to the energy for the reordering of grain boundaries in the UFG material [34, 35]. The activation energy of 260 kJ/mol found for temperatures higher than 698K is close to self-diffusion of Fe, and can be correlated to the lattice diffusion. It should be pointed out that the value Q obtained in the current study at high temperatures regime is significantly higher than nanocrystalline pure iron alpha [7].

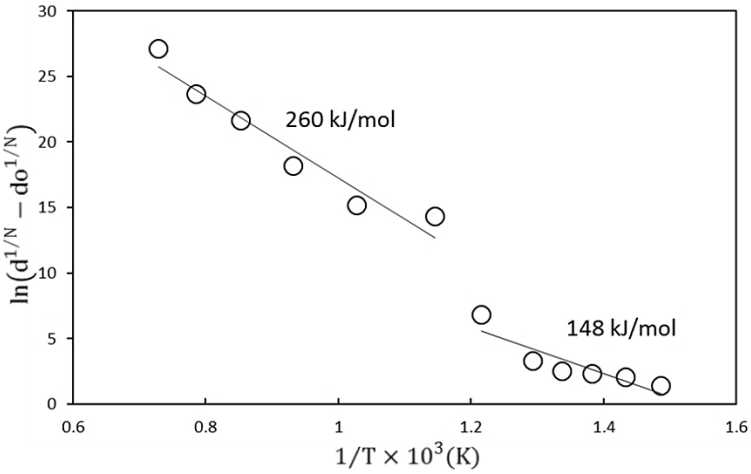

Figure 6. Graph of $ln(\left(d^{1/N} - d_o^{1/N}\right)$ versus *1/T* for determining the activation grain growth

The decrease of dislocation density in low annealing temperatures was reported in pure iron [34, 35]. It happened due to the partial annihilation of stored dislocation by the recovery process and the change from non-equilibrium grain boundaries to equilibrium grain boundaries and the relaxation of internal elastic stress [34, 36, 37].

Because of the character and mobility of the boundaries, the recovery stage is the main point in the annealing process [22, 38]. The extended recovery stage relates to the softening of the material [35]. After the annealing temperature reached 698K, the microstructure showed homogeneous grain coarsening with grain appearance comparable with the ECAP processed structure. It can be summarized that the annealing process of an ultrafine-grained iron-chromium alloy can be regarded as two-stage homogeneous normal grain growth with two levels of activation energy.

CONCLUSIONS

The effect of the annealing behaviour on a UFG iron-chromium alloy as BCC metallic material by ECAP was studied focusing on the residual dislocation-related strain on the early stage of grain growth. The softening of a material occurred in the typical three stages, comprised of recovery with constant hardness, and subsequent significant softening accompanying homogeneous grain-growth, and the final slow grain growth with little change of hardness. The extended recovery stage was confirmed by XRD prior to the appreciable grain-growth. The microstructure of the recovery stage shows homogeneous coarsened grain with grain appearance comparable with the ECAP processed structure. The pure BCC material showed the release strain energy stored as dislocations density in recovery process prior to the recrystallization process. In this regard, the strain energy that was stored in UFG structure was released earlier and this early recovery of strain affected the mode grain growth in annealing.

ACKNOWLEDGEMENTS

The authors gratefully acknowledge the financial support of a Grant-in-Aid for Scientific Research on Innovative Areas “Bulk nano metals,” MEXT Japan (No 25102710).

REFERENCES

[1] R. Z. Valiev, Y. Estrin, Z. Horita, T. G. Langdon, M. J. Zehetbauer, and Y. T. Zhu, “Fundamentals of superior properties in bulk NanoSPD materials,” *Mater. Res. Lett.*, vol. 4, no. 1, pp. 1–21, 2016.

[2] Y. Estrin and A. Vinogradov, “Extreme grain refinement by severe plastic deformation: A wealth of challenging science,” *Acta Mater.*, vol. 61, no. 3, pp. 782–817, 2013.

[3] X. Sauvage, G. Wilde, S. V. Divinski, Z. Horita, and R. Z. Valiev, “Grain boundaries in ultrafine grained materials processed by severe plastic deformation and related phenomena,” *Mater. Sci. Eng. A*, vol. 540, pp. 1–12, 2012.

[4] A. Fattah-alhosseini, O. Imantalab, Y. Mazaheri, and M. K. Keshavarz, “Microstructural evolution, mechanical properties, and strain hardening behavior of ultrafine grained commercial pure copper during the accumulative roll bonding process,” *Mater. Sci. Eng. A*, vol. 650, pp. 8–14, 2016.

[5] Y. Chen, N. Gao, G. Sha, S. P. Ringer, and M. J. Starink, “Microstructural evolution, strengthening and thermal stability of an ultrafine-grained Al-Cu-Mg alloy,” *Acta Mater.*, vol. 109, pp. 202–212, 2016.

[6] Y. Xirong, Z. Xicheng, and F. Wenjie, “Deformed Microstructures and Mechanical Properties of CP-Ti Processed by Multi-Pass ECAP at Room Temperature,” *Rare Met. Mater. Eng.*, vol. 38, no. 6, pp. 955–957, Jun. 2009.

[7] Y. Okitsu, N. Takata, and N. Tsuji, “Dynamic deformation behavior of ultrafine-grained iron produced by ultrahigh strain deformation and annealing,” *Scr. Mater.*, vol. 64, no. 9, pp. 896–899, 2011.

[8] Y. G. Ko and K. Hamad, “Analyzing the thermal stability of an ultrafine grained interstitial free steel fabricated by differential speed rolling,” *Mater. Sci. Eng. A*, vol. 726, pp. 32–36, 2018.

[9] M. H. Razmpoosh, A. Zarei-Hanzaki, N. Haghdadi, J. H. Cho, W. J. Kim, and S. Heshmati-Manesh, “Thermal stability of an ultrafine-grained dual phase TWIP steel,” *Mater. Sci. Eng. A*, vol. 638, pp. 5–14, 2015.

[10] N. Kumar and R. S. Mishra, “Thermal stability of friction stir processed ultrafine grained AlMgSc alloy,” *Mater. Charact.*, vol. 74, pp. 1–10, Dec. 2012.

[11] M. Kawasaki, Z. Horita, and T. G. Langdon, “Microstructural evolution in high purity aluminum processed by ECAP,” *Mater. Sci. Eng. A*, vol. 524, no. 1–2, pp. 143–150, 2009.

[12] M. Rifai, H. Miyamoto, and H. Fujiwara, “Effects of Strain Energy and Grain Size on Corrosion Resistance of Ultrafine Grained Fe-20 % Cr Steels with Extremely low C and N Fabricated by ECAP,” *Int. J. Corros.*, vol. 2015, no. 1, pp. 1–9, 2015.

[13] S. H. He, K. Y. Zhu, and M. X. Huang, “A unified dislocation-based model for ultrafine- and fine-grained face-centered cubic and body-centered cubic metals,” *Comput. Mater. Sci.*, vol. 131, pp. 1–10, 2017.

[14] H. Fan, S. Liu, C. Deng, X. Wu, L. Cao, and Q. Liu, “Quantitative analysis: How annealing temperature influences recrystallization texture and grain shape in tantalum,” *Int. J. Refract. Met. Hard Mater.*, vol. 72, pp. 244–252, 2018.

[15] M. El-Tahawy *et al.*, “Stored energy in ultrafine-grained 316L stainless steel processed by high-pressure torsion,” *J. Mater. Res. Technol.*, vol. 6, no. 4, pp. 339–347, 2017.

[16] M. A. Vicente Alvarez, J. R. Santisteban, P. Vizcaíno, G. Ribárik, and T. Ungar, “Quantification of dislocations densities in zirconium hydride by X-ray line profile analysis,” *Acta Mater.*, vol. 117, pp. 1–12, 2016.

[17] Y. Iwahashi, J. Wang, Z. Horita, M. Nemoto, and T. G. Langdon, “PRINCIPLE OF EQUAL-CHANNEL ANGULAR PEESSING FOR THE PROCESSING OF ULTRA-FINE GRAINED MATERIALS,” *Scr. Mater.*, vol. 35, no. 2, pp. 143–146, 1996.

[18] N. A. Raji and O. O. Oluwole, “Recrystallization Kinetics and Microstructure Evolution of Annealed Cold-Drawn Low-Carbon Steel,” *J. Cryst. Process Technol.*, vol. 03, no. 04, pp. 163–169, 2013.

[19] N. P. Gurao and S. Suwas, “Effect of Phase Contiguity and Morphology on the Evolution of Deformation Texture in Two-Phase Alloys,” *Metall. Mater. Trans. A Phys. Metall. Mater. Sci.*, vol. 48, no. 2, pp. 809–827, 2017.

[20] M. Rifai, R. Haga, H. Miyamoto, and H. Fujiwara, "Microstructural Development of Fe-20mass % Cr Alloys and Pure Copper Processed by Equal-Channel Angular Pressing," vol. 2013, no. April, pp. 1–8, 2013.

[21] J. V Sharp, M. J. Makin, and J. W. Christian, "Dislocation Structure in Deformed Single Crystals of Magnesium," *Phys. Status Solidi*, vol. 11, pp. 845–864, 1965.

[22] F. J. Humphreys, P. B. Prangnell, J. R. Bowen, A. Gholinia, and C. Harris, "Developing stable fine − grain microstructures by large strain deformation Developing stable fine-grain microstructures by large strain deformation," *Philos. Trans. R. Soc. A Math. Phys. Eng. Sci.*, no. June, pp. 1663–1681, 1999.

[23] S. Z. Han, M. Goto, J.-H. Ahn, S. H. Lim, S. Kim, and J. Lee, "Grain growth in ultrafine grain sized copper during cyclic deformation," *J. Alloys Compd.*, vol. 1, pp. 10–12, Dec. 2013.

[24] E. Tohidlou and A. Bertram, "Effect of initial orientation on subgrain formation in nickel single crystals during equal channel angular pressing," *Mech. Mater.*, vol. 114, pp. 30–39, 2017.

[25] C. Sun *et al.*, "Thermal stability of ultrafine grained Fe–Cr–Ni alloy," *Mater. Sci. Eng. A*, vol. 542, pp. 64–70, Apr. 2012.

[26] A. A. Nazarov and R. T. Murzaev, "Nonequilibrium grain boundaries and their relaxation under oscillating stresses in columnar nickel nanocrystals studied by molecular dynamics," *Comput. Mater. Sci.*, vol. 151, no. May, pp. 204–213, 2018.

[27] J. A. Muñoz, O. F. Higuera, and J. M. Cabrera, "Microstructural and mechanical study in the plastic zone of ARMCO iron processed by ECAP," *Mater. Sci. Eng. A*, vol. 697, no. May, pp. 24–36, 2017.

[28] Z. J. Zheng, J. W. Liu, and Y. Gao, "Achieving high strength and high ductility in 304 stainless steel through bi-modal microstructure prepared by post-ECAP annealing," *Mater. Sci. Eng. A*, vol. 680, pp. 426–432, 2017.

[29] K. Huang and R. E. Logé, "A review of dynamic recrystallization phenomena in metallic materials," *Mater. Des.*, vol. 111, pp. 548–574, 2016.

[30] H. R. R. Ashtiani and P. Karami, "Prediction of the Microstructural Variations of Cold-Worked Pure Aluminum during Annealing Process," *Model. Numer. Simul. Mater. Sci.*, vol. 05, no. 01, pp. 1–14, 2015.

[31] H. Miyamoto, T. Xiao, and T. Uenoya, "Facilitated Recrystalization of the Hard-to-Recrystalize Structure in 16% Cr Steel Sheets by one-Pass ECAP Prior to Cold Rolling," *Mater. Sci. Forum*, vol. 702–703, pp. 607–610, 2011.

[32] H. R. Peng, M. M. Gong, Y. Z. Chen, and F. Liu, "Thermal stability of nanocrystalline materials: thermodynamics and kinetics," *Int. Mater. Rev.*, vol. 62, no. 6, pp. 303–333, 2017.

[33] I. Roy, M. Chauhan, and E. J. Lavernia, "Thermal Stability in Bulk Cryomilled Ultrafine-Grained 5083 Al Alloy," *Metall. Mater. Trans. A*, vol. 37, no. March, pp. 721–730, 2006.

[34] S. S. Hazra, A. a. Gazder, and E. V. Pereloma, "Stored energy of a severely deformed interstitial free steel," *Mater. Sci. Eng. A*, vol. 524, no. 1–2, pp. 158–167, Oct. 2009.

[35] R. D. Doherty *et al.*, "Current issues in recrystallization : a review," *Mater. Sci. Eng. A*, vol. 238, pp. 219–274, 1997.

[36] N. A. Alang, "Characterization of creep deformation and rupture behaviour of P92 steel weldment at 600°C N.A.," *J. Mech. Eng. Sci.*, vol. 12, no. 3, pp. 3976–3987, 2018.

[37] M. Z. O. C. F. Adnan, Z. Sajuri, "Effect of uniaxial load on microstructure and mechanical properties of Thixo-joint AISI D2 tool steel," *J. Mech. Eng. Sci.*, vol. 13, no. 2, pp. 5006–5020, 2019.

[38] T. D. W. and A. H. S. M. Zaimi, M. N. Azran, M. S. Kasim, M. R. M. Kamal, I. S. Othman, N. Mohamad, K. T. Lau, "Effect of heat treatment on the tribological performance of electroless quaternary nickel alloy," *J. Mech. Eng. Sci.*, vol. 13, no. 3, pp. 5637–5652, 2019.